Mode coupling and polar nanoregions in the relaxor ferroelectric $Pb(Mg_{1/3}Nb_{2/3})O_3$

S. Wakimoto,[1,2,*] C. Stock,[2] Z.-G. Ye,[3] W. Chen,[3] P. M. Gehring,[4] and G. Shirane[1]
[1]*Department of Physics, Brookhaven National Laboratory, Upton, New York 11973*
[2]*Department of Physics, University of Toronto, Toronto, Ontario, Canada M5S 1A7*
[3]*Department of Chemistry, Simon Fraser University, Burnaby, British Columbia, Canada V5A 1S6*
[4]*NIST Center for Neutron Research, National Institute of Standards and Technology, Gaithersburg, Maryland 20899*
(Received 9 August 2002; published 6 December 2002)

We present a quantitative analysis of the phonon line shapes obtained by neutron inelastic scattering methods in the relaxor ferroelectric $Pb(Mg_{1/3}Nb_{2/3})O_3$ (PMN). Differences in the shapes and apparent positions of the transverse acoustic– (TA) and transverse optic– (TO) phonon peaks measured in the (300) and (200) Brillouin zones at 690 K are well described by a simple model that couples the TA and soft TO modes in which the primary parameter is the wave vector and temperature-dependent TO linewidth $\Gamma(q,T)$. This mode-coupling picture provides a natural explanation for the uniform displacements of the polar nanoregions (PNR's), discovered by Hirota *et al.* as the PNR result from the condensation of a soft TO mode that also contains a large acoustic component.

DOI: 10.1103/PhysRevB.66.224102 PACS number(s): 77.84.Dy, 61.12.−q, 77.80.Bh, 64.70.Kb

I. INTRODUCTION

Considerable advances have been made over the past several years in our understanding of the lattice dynamics of the relaxor ferroelectric $Pb(Mg_{1/3}Nb_{2/3})O_3$ (PMN), which is a prototypical member of a class of compounds that possesses exceptional piezoelectric properties and an unusually broad and frequency-dependent dielectric susceptibility that peaks at a temperature T_{max} ($\approx$265 K at 1 kHz for PMN).[1] Pioneering neutron scattering work on PMN in 1999 by Naberezhnov *et al.*[2] has been followed by a systematic series of neutron scattering experiments by Gehring *et al.*[3–6] and Wakimoto *et al.*[7] The results of these latter measurements have firmly established the existence of significant soft mode dynamics in PMN. In particular, they have demonstrated a linear temperature dependence of the zone-center soft phonon energy squared $(\hbar\omega_0)^2$ over a wide temperature range, as shown in Fig. 1.

A fundamental feature that appears common to all relaxors is that of the polar nanoregions (PNR's). The presence of these regions was inferred in 1983 by Burns and Dacol, who found that the optic index of refraction of PMN deviates from a linear temperature dependence at a temperature $T_d \approx 620$ K that is far above T_{max}.[8] In conventional ferroelectrics this deviation corresponds to a uniform polarization that only develops below T_c. Given the absence of any net polarization in PMN at T_d, the optical data indicate the formation of tiny regions of local and randomly oriented polarization that were speculated to originate in Nb-rich parts of the crystal several unit cells in size. The dynamical effects of these PNR are clearly manifest in neutron scattering measurements. Gehring *et al.* have found that the long-wavelength transverse optic (TO) phonons are heavily damped below T_d, which gives rise to the anomalous ''waterfall'' feature.[6] Neutron scattering measurements further suggest that the appearance of the PNR at T_d is accompanied by a remarkable overdamping of the zone center ($q=0$) TO phonons. As shown in Fig. 1(a), the zone-center TO phonon linewidth broadens with decreasing temperature until finally at T_d no discernible phonon peak remains. It has subsequently been reported that the overdamped zone-center TO mode reappears below $\sim$220 K.[7]

The formation of the PNR at T_d is the most important aspect of the relaxor problem, and it is intriguing that it is accompanied not only by the overdamping of the zone-center TO soft mode, but also by the appearance of diffuse scattering. The Brillouin zone dependence of the neutron diffuse scattering intensities has been extensively measured by Vakhrushev *et al.*[9,10] and later it was shown by Naberezhnov *et al.* that the onset of the diffuse scattering occurs at T_d.[2] The coincidence of these phenomena at T_d point to a picture in which the PNR result from the condensation of the soft TO mode. If this picture is correct, then the atomic displacements associated with the diffuse scattering must match those associated with the soft TO phonon, namely, they must satisfy the center-of-mass condition. However, the diffuse scattering intensities in different Brillouin zones are entirely inconsistent with the TO-phonon intensities. This longstanding puzzle was resolved recently by Hirota *et al.*[11] By calculating the dynamic structure factor with the assumption that the soft TO mode condenses with an additional uniform shift of all atoms, they demonstrated that the intensities of TO phonons and diffuse scattering can be completely reconciled. Their calculation shows that this uniform shift δ_{shift} is comparable to the displacement due to the TO mode condensation $\delta_{c.m.}$, and that δ_{shift} is 60% of the displacement of the Pb atom. While the origin of this uniform phase shift is unknown, the success of the model provides further support to the idea connecting the PNR and the soft mode.

In this paper we demonstrate that a simple model that couples the transverse acoustic and soft optic modes, similar to that used by Harada *et al.* to describe the asymmetric phonon line shapes found in $BaTiO_3$,[12] is able to reproduce the phonon line shapes observed in PMN in both the (200) and (300) Brillouin zones, which exhibit very different scattering profiles. This naturally implies that a condensation at T_d of a *coupled* TO mode would then contain a TA component, and

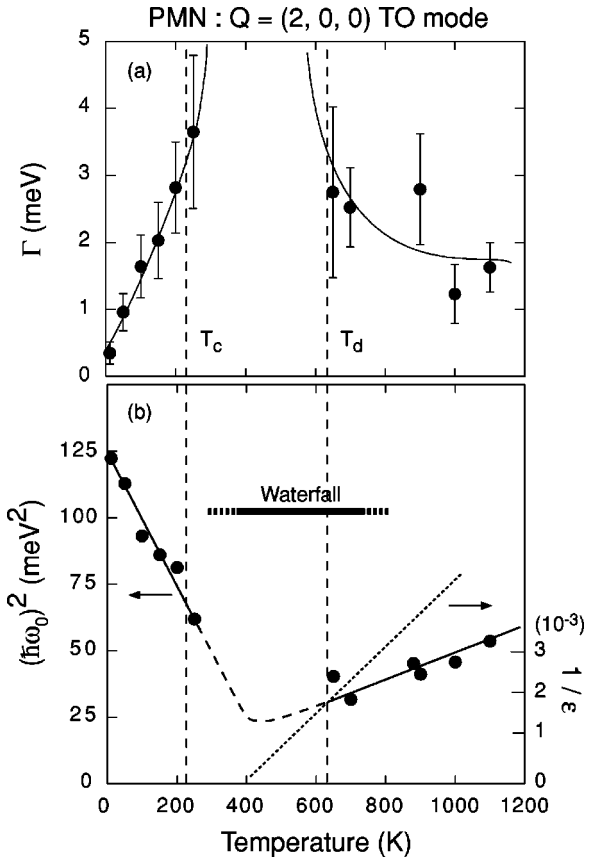

FIG. 1. (a)Temperature dependence of the (2,0,0) zone-center TO-phonon linewidth Γ_1. Above T_d Γ_1 increases gradually with decreasing temperature, whereas below T_c it decreases rapidly. For temperatures between T_c and T_d it is impossible to determine the linewidth due to the overdamped nature of the TO mode. Solid lines are guides to the eye. (b) Temperature dependence of the (2,0,0) zone-center TO-phonon energy squared $(\hbar\omega_0)^2$ from Ref. 13. The dotted line shows the Curie-Weiss behavior of the dielectric constant $1/\epsilon \propto T - T_0$ with $T_0 = 400$ K reported by Viehland *et al.*

this might closely relate to the uniform phase shift reported by Hirota *et al.*[11]

II. EXPERIMENTAL DETAILS

Single crystals of PMN were grown using a top-seeded solution method with PbO as flux. Two crystals were chosen for the neutron scattering experiments. One has a volume of 0.09 cm^3 and a mass of 0.74 g, and the other has a volume of 0.40 cm^3 and a mass of 3.25 g (the density of PMN is 8.13 g/cm^3). Since both samples show quantitatively similar results, we will not distinguish between the two samples in this paper.

Our neutron scattering experiments were performed at the BT9 triple-axis spectrometer located at the NIST Center for Neutron Research. The (002) reflection of highly oriented pyrolytic graphite (HOPG) crystals was used to monochromate the incident neutron energy E_i and to analyze final neutron energy E_f. The data were taken with a fixed final energy $E_f = 14.7$ meV ($\lambda = 2.36$ Å) and horizontal collimations of 40′-40′-*S*-40′-80′ (S denotes sample) between source and detector. An HOPG filter was placed after the analyzer to eliminate higher-order wavelength contamination in the scattered beam. The crystal was placed with a natural $\{100\}_{\text{cubic}}$ facet facing down onto a boron nitride post, and held in place with tantalum wire. This orientation allows access to $(h0l)$-type reflections in the horizontal scattering plane. The mosaic spreads of the crystals were less than 24′ at the (200) reflection, which is resolution limited with the above configuration, and indicate a high crystal quality. The room temperature lattice constant is 4.04 Å; therefore one reciprocal lattice unit (r.l.u.) equals 1.553 $Å^{-1}$.

PMN reportedly remains cubic down to 5 K.[13] Consistent with this observation, we find no definitive evidence of a structural transition in the temperature range $50 \leqslant T \leqslant 400$ K. On the other hand, a macroscopic ferroelectric state can be established in PMN by cooling it in a moderate ($E = 1.7$ kV/cm) applied electric field. The induced polarization then vanishes upon warming above $T_c = 213$ K as a first-order phase transition.[1] To date, the aforementioned reappearance of the zone-center TO mode, which also coincides with the disappearance of the TA-phonon broadening,[7] is the most direct evidence of ferroelectric ordering in zero field associated with T_c. Other anomalies have also been reported near T_c, such as the sharp peak in the temperature dependence of the hypersonic damping reported by Tu *et al.*[14] and the abrupt change in the thermal expansion of the lattice parameter observed by Dkhil *et al.*[15] To pursue this issue more carefully, we looked for subtle structural changes near T_c by employing a tighter sequence of horizontal collimations (40′-10′-*S*-10′-80′) to improve the instrumental q resolution. Figure 2 shows the temperature dependence of the (2,0,2) Bragg peak width along the (a) [101] (longitudinal) and (b) $[10\bar{1}]$ (transverse) directions. If PMN were to transform from a cubic to a rhombohedral structure, then the (2,0,2) Bragg peak would split along the longitudinal direction. However, we observed neither a splitting nor a broadening of the (2,0,2) Bragg peak along [101]. Figures 2(c) and 2(d) show longitudinal scans of the (2,0,2) Bragg peak measured at 300 and 50 K. The peak width is almost resolution limited for $50 \leqslant T \leqslant 300$ K. Instead, we observed a small, but clear, jump in the transverse width at T_c, which is shown in Fig. 2(b). However, we did not observe a corresponding enhancement of the peak intensity below T_c that is normally expected at a structural phase transition due to the release of primary extinction.

III. MODE-COUPLING MODEL CROSS SECTION

The neutron inelastic scattering technique provides a direct measure of the scattering function $S(\mathbf{q},\omega)$, as this is simply related to the experimentally measured scattering cross section. More importantly, $S(\mathbf{q},\omega)$ is related to the imaginary part of the dynamic susceptibility $\chi''(\mathbf{q},\omega)$ via the fluctuation-dissipation theorem

$$S(\mathbf{q},\omega) = \{1 + n(\omega)\}\chi''(\mathbf{q},\omega), \tag{1}$$

where $n(\omega)$ is the Bose factor $(e^{\omega/k_BT} - 1)^{-1}$. By choosing the scattering vector $\mathbf{Q} = \mathbf{G} + \mathbf{q}$, where $\mathbf{G}$ is a reciprocal lat-

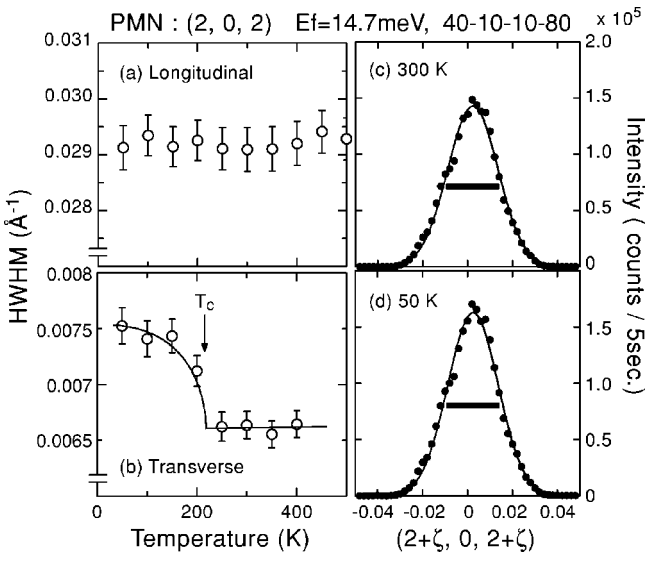

FIG. 2. Temperature dependence of the (2,0,2) Bragg peak linewidth measured along the (a) [101] (longitudinal), and (b) $[10\bar{1}]$ (transverse) directions. If the system transforms from a cubic to a rhombohedral phase, then the (2,0,2) peak should split along the longitudinal direction. Instead, only the transverse scan shows a clear change near T_c. For ease of comparison, panels (c) and (d) show the (2,0,2) line shape measured along the longitudinal direction at 300 and 50 K. The solid bars represent the instrumental longitudinal q resolution.

tice vector and **q** is a phonon wave vector, one can measure the phonon dispersions in different Brillouin zones. The measurements reported here were made at $\mathbf{G}=(2,0,0)$ and $(3,0,0)$. However, a model cross section is required in order to extract meaningful parameters from the measurements, and to correct for the effects of the instrumental resolution. The form we chose for $S(\mathbf{q},\omega)$ is discussed by Harada *et al.*[12] and pertains to a system in which a coupling exists between two vibrational modes. In this case we have

$$S(\mathbf{q},\omega)=\{1+n(\omega)\}\frac{\omega}{A^2+\omega^2B^2}\{[(\Omega_2^2-\omega^2)B-\Gamma_2A]F_1^2 + 2\lambda BF_1F_2+[(\Omega_1^2-\omega^2)B-\Gamma_1A]F_2^2\}, \quad (2)$$

where

$$A=(\Omega_1^2-\omega^2)(\Omega_2^2-\omega^2)-\omega^2\Gamma_1\Gamma_2-\lambda^2, \quad (3)$$

$$B=\Gamma_1(\Omega_2^2-\omega^2)+\Gamma_2(\Omega_1^2-\omega^2). \quad (4)$$

The model parameters Ω, Γ, F, and λ represent the phonon frequency, damping, dynamic structure factor, and coupling constant, while the indices 1 and 2 denote the TO and TA modes, respectively. Hereafter, we shall refer to this as the mode-coupling (MC) function. This function shows larger coupling effects the closer the TO and TA frequencies become, or the more heavily damped either mode becomes. In the Appendix we identify several important features of the MC function that can produce large differences in the phonon profiles.

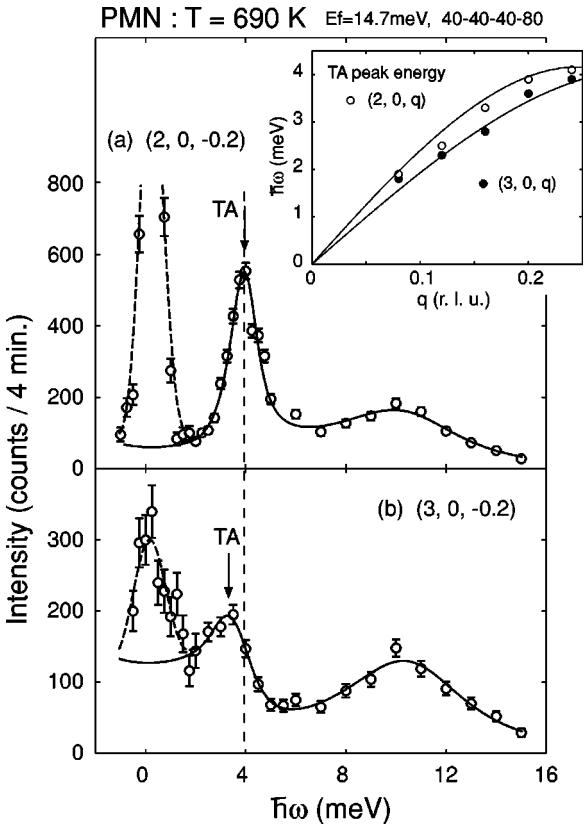

FIG. 3. Constant-**Q** scans measured at (a) $\mathbf{Q}=(2,0,-0.2)$ and (b) $\mathbf{Q}=(3,0,-0.2)$ at 690 K. Solid lines are fits to the mode-coupling function convoluted with the instrumental resolution function. A negative F_1F_2 is used for $(2,0,-0.2)$ while a positive F_1F_2 is used for $(3,0,-0.2)$. Although the scattering intensities from the TA modes peak at different frequencies, the fits yield the same value for $\Omega_2=4.2$ (as is required), as well as the same value for $\lambda=17$. Note that the TA structure factor $|F_2|^2$ at $(3,0,-0.2)$ is ≈ 100 times smaller than it is at $(2,0,-0.2)$. The inset shows the *apparent* phonon frequencies of the TA modes determined solely from the peak position. The TA modes at $(3,0,q)$ appear systematically at lower frequency than do those at $(2,0,q)$.

IV. NEUTRON SCATTERING EXPERIMENTAL RESULTS

A. Phonon profiles at 690 K

Substantial differences between the phonon profiles obtained in the $(2,0,q)$ and $(3,0,q)$ Brillouin zones are apparent in Fig. 3, which displays typical data sets for $q=-0.2$ measured at 690 K. A major difference is that the scattering associated with the TA phonon appears to peak at different energies, i.e., the TA energy seems lower at $(3,0,-0.2)$ than it is at $(2,0,-0.2)$. This difference is systematically observed at different q positions as shown in the inset of Fig. 3, where the apparent TA-phonon energies obtained from the peak position are plotted as a function of q in the (200) and (300) zones at 690 K. The solid lines are merely guides to the eye. As is clearly seen, the TA mode energies in the (300) zone are consistently lower than those in (200) at all values of q studied. Of course, for a crystal that possesses true long-range translational order, all phonon energies in different Brillouin zones must be identical.

TABLE I. Parameters obtained from the fit of the 690 K data to the MC function.

Q	Ω_1	Ω_2	Γ_1	Γ_2	$\lvert F_1\rvert$	$\lvert F_2\rvert$	λ
(2,0,−0.2)	10.85	4.30	6.10	0.79	27.0	13.1	17.4
(3,0,−0.2)	10.92	4.20	6.05	1.95	27.0	1.09	17.4
(3,0,−0.12)	9.05	2.67	7.77	0.69	25.7	<0.5	7.21
(3,0,−0.08)	8.76	1.92	13.1	0.03	31.3	0.64	1.88

When fitting these phonon profiles with the MC function, we found that a change in the sign of the product of the dynamic structure factors F_1F_2 can reconcile the discrepancies in the TA-phonon peak position. Specifically, if we set $F_1F_2<0$ for (2,0,−0.2) and $F_1F_2>0$ for (3,0,−0.2), we obtain the same TA-phonon energy Ω_2 for each zone. This occurs because for positive F_1F_2 the spectral weight of the TO mode increasingly shifts to the region below the TA mode energy Ω_2 with increasing TO mode damping Γ_1, whereas for negative F_1F_2 this spectral weight shifts to the region between the TO and TA mode energies. Thus the MC function produces a higher (lower) apparent TA phonon energy for negative (positive) F_1F_2, even though Ω_2 is always the same. Further details are given in the Appendix. The fits to the MC function include an additional Gaussian component, which is used to describe the elastic incoherent peak at $\hbar\omega=0$. The fitted curves are shown in Fig. 3, where the solid and dashed lines correspond to the MC and Gaussian functions, respectively. The fitting parameters are listed in Table I. It is satisfying to note that the values for Ω and Γ derived from the fits of both the (2,0,−0.2) and (3,0,−0.2) phonon profiles agree quite well, even though the apparent TA peak positions are different.

Another important difference between the (200) and (300) zones is that the dynamic structure factor $\lvert F_2\rvert$ at (3,0,−0.2) is about ten times smaller than that for (2,0,−0.2). This fact is readily confirmed since, for wave vectors close to the zone center, the ratio of $\lvert F_2\rvert$ in two different zones should agree with that for $\lvert F_N\rvert$, the nuclear static structure factor. This is given by

$$F_N(\mathbf{Q})=\sum_j b_j e^{i\mathbf{Q}\cdot\mathbf{d}_j}e^{-W_j}, \tag{5}$$

where b_j, $\mathbf{d}_j$, and e^{-W_j} are the neutron scattering length, atomic coordination vector, and the Debye-Waller factor for the jth atom, respectively. In fact, this formula gives $\lvert F_N(200)\rvert/\lvert F_N(300)\rvert=11.2$, which is in excellent agreement with the value $\lvert F_2(2,0,-0.2)\rvert/\lvert F_2(3,0,-0.2)\rvert=12.0$ obtained from the fits. This implies, however, that the actual intensity of the TA mode at (3,0,−0.2) (which is proportional to $\lvert F_2\rvert^2$) should be over 100 times smaller than that at (2,0,−0.2). Yet the TA peak is clearly visible at (3,0,−0.2). This can also be explained by the MC function, since the intensity of the TO mode is transferred to the TA mode due to the coupling, which in turn produces an enhancement of the TA cross section. This feature is also described in more detail in the Appendix.

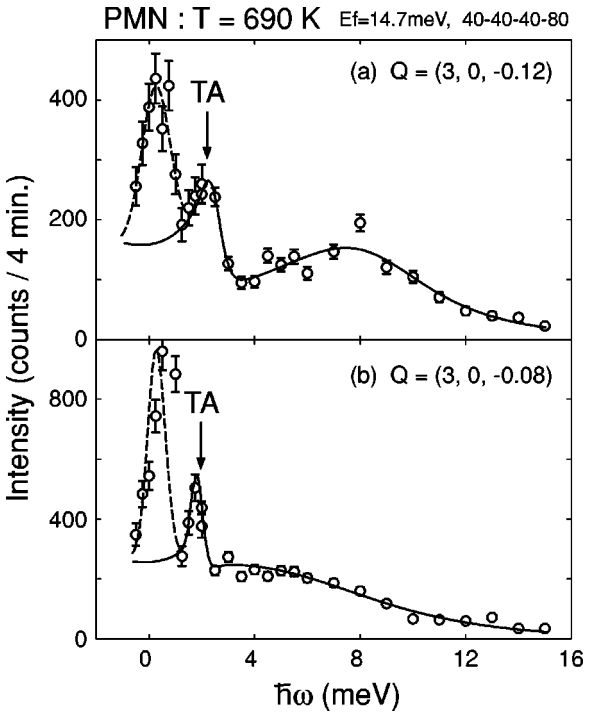

FIG. 4. Constant-**Q** scans measured at (a) **Q**=(3,0,−0.12) and (b) **Q**=(3,0,−0.08). Solid lines are fits to the mode-coupling function convoluted with the instrumental resolution function. Here F_1F_2 was chosen to be positive for both scans. All parameter values are listed in Table I.

Features similar to those discussed above are also found in the phonon profiles at smaller q. Data taken at (3,0,−0.12) and (3,0,−0.08) are shown in Figs. 4(a) and 4(b), along with the fits to the MC function. As before, the solid and dashed lines correspond to MC and Gaussian functions, respectively. The fitting parameters are listed in Table I. The coupling constant λ was determined such that Ω_1 and Ω_2 are equal in each zone. At smaller q, the parameter Γ_1 becomes larger, meaning that the TO mode is more heavily damped. This is consistent with the "waterfall" picture. We have thus shown that the phonon profiles in both the (200) and (300) Brillouin zones can be explained satisfactorily by the MC function at all q. However there is still an open question. While we know that λ decreases at smaller q, we do not yet have a specific model that describes the q dependence of λ.

B. Temperature dependence of the phonon cross section

To check the consistency of our model, we have analyzed the TA-phonon profiles at (3,0,−0.2) at different temperatures. Before showing the results for (3,0,−0.2), we first present the temperature dependence of the phonon profiles obtained at (2,0,−0.2). These are displayed in the left panel of Fig. 5 at (a) 700 K, (b) 500 K, and (c) 290 K. Each profile has been fitted to a resolution-convoluted MC function plus a Gaussian centered at $\hbar\omega=0$ with $F_1F_2<0$. The fitted parameter values are listed in Table II. Consistent with the results of the previous section, $\lvert F_1\rvert/\lvert F_2\rvert\approx 2$ at 700 K, and is

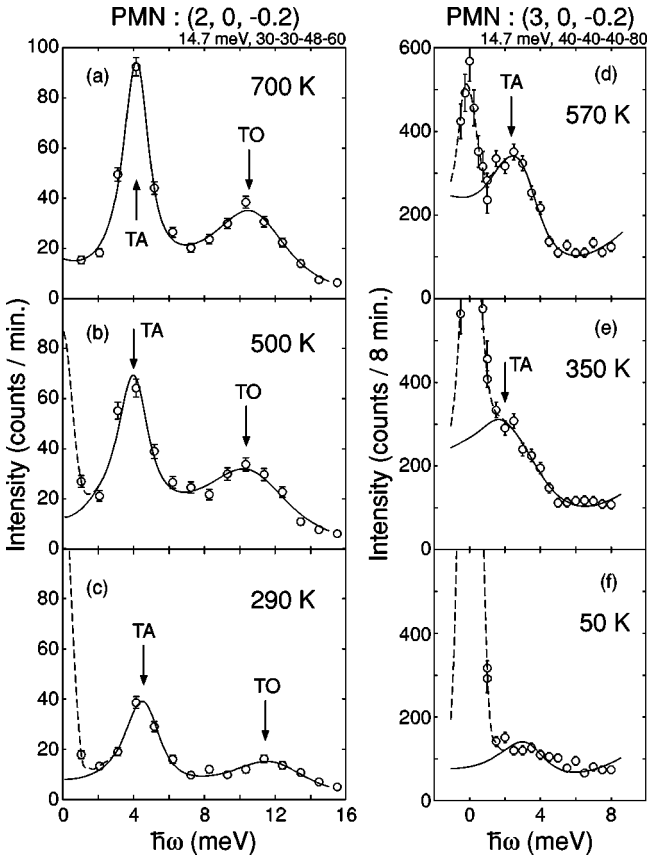

FIG. 5. The left panel shows phonon profiles measured at $\mathbf{Q}=(2,0,-0.2)$ at (a) 700 K, (b) 500 K, and (c) 290 K. The right panel shows TA-phonon profiles measured at $\mathbf{Q}=(3,0,-0.2)$ at (d) 570 K, (e) 350 K, and (f) 50 K. The lines, except those shown in (f), represent fits to the resolution-convoluted MC function plus a Gaussian function centered at $\hbar\omega=0$. The solid and dashed lines correspond to the MC and Gaussian cross sections, respectively. The solid line in (f) is an MC cross section using the same parameters as those obtained in (d).

almost independent of temperature down to 290 K. Similarly, Ω_1, Ω_2, and λ are also independent of temperature. On the other hand, Γ_2 (the TA mode linewidth) is larger at 500 and 290 K, which is consistent with the TA linewidth broadening below T_d reported in Ref. 7. The linewidth of the TO mode Γ_1 is also slightly broader below 700 K.

The right panel of Fig. 5 shows the temperature dependence of the TA phonon for $\mathbf{Q}=(3,0,-0.2)$ measured at (d) 570 K, (e) 350 K, and (f) 50 K. Because these data do not include the TO mode, the profiles for 570 and 350 K were fitted fixing $\Omega_1=11.2$, $\Gamma_1=6$, and $\lambda=17.4$, while $F_1F_2>0$. Consequently, the uncertainties associated with the parameters in this zone will be larger. Values for the fitted parameters are listed in Table II. From this analysis we find that the ratio $|F_1(200)|/|F_1(300)|\approx 1$. Since the nuclear structure factor calculations imply $|F_2(200)|/|F_2(300)|\approx 10$, and we know that $|F_1(200)|/|F_2(200)|\approx 2$, we can estimate that $|F_1(300)|/|F_2(300)|\approx 20$. This agrees reasonably well with the fitted ratio $|F_1|/|F_2|\approx 16$ at both temperatures, and represents a reassuring self-consistency check of our model. Moreover, a broadening of the TA mode is found

TABLE II. Parameters obtained from the fit of the data in Fig. 5 to the MC function.

Q	T(K)	Ω_1	Ω_2	Γ_1	Γ_2	$\lvert F_1\rvert$	$\lvert F_2\rvert$	λ
(2,0,−0.2)	700	11.1	4.60	5.24	1.24	10.5	5.65	17.4
	500	11.1	4.45	6.07	1.70	12.5	6.07	16.8
	290	12.0	4.90	5.96	1.52	11.5	6.04	17.9
(3,0,−0.2)	570	11.2	3.90	6.00	2.89	12.1	0.78	17.4
	350	11.2	4.29	6.00	4.81	14.0	0.82	17.4

at $(3,0,-0.2)$ that is qualitatively similar to that observed at $(2,0,-0.2)$. Thus, the temperature dependence of the phonon profiles is consistent with the mode-coupling model. However we did not obtain a clear TA phonon peak at 50 K. Instead, the solid line shown in Fig. 5(f) represents the profile that would be expected for the TA mode assuming the same parameters as those obtained from fits to the 570 K data. The agreement between the data and fit in this case is quite good.

C. Dynamic structure factor of the TO phonon

The ratio of the dynamic structure factors that govern the transverse optic phonon intensities in different Brillouin zones depends on the associated atomic vibrational displacements. Two of the most important atomic vibrational modes are those proposed by Slater and Last, and are discussed by Harada *et al.*[16] The Slater mode corresponds to atomic motions in which the oxygen and Mg/Nb atoms move in opposition while the Pb atoms remain stationary. The Last mode corresponds to opposing motions of the Pb atoms and rigid $(Mg/Nb)O_6$ octahedra. The dynamic structure factor is given by

$$F_{\text{inel}}=\sum_j [\mathbf{Q}\cdot\boldsymbol{\xi}_j]b_j e^{i\mathbf{G}\cdot\mathbf{d}_j}e^{-W_j}, \tag{6}$$

where $\boldsymbol{\xi}_j$ is the normalized displacement vector for the jth atom. Assuming only the Slater and Last modes are significant, then $\boldsymbol{\xi}_j$ can be written in terms of the atomic displacement vectors for the Slater ($\mathbf{s}_{j1}$) and Last ($\mathbf{s}_{j2}$) modes, and the parameter S, which is a measure of the relative contributions of the Last and Slater modes, as follows:

$$\boldsymbol{\xi}_j=\mathbf{s}_{j1}+\mathbf{S}\mathbf{s}_{j2}. \tag{7}$$

For PMN, Hirota *et al.*[11] calculated the value of $|F_{\text{inel}}|^2$ for $-0.5\leqslant S\leqslant 2$ at (200), (300), and (110) as shown in Fig. 6 of Ref. 11. Our result of $|F_1(200)|/|F_1(300)|\approx 1$ obtained from our fits to the MC function is consistent with the value $S=1.5$ determined by Hirota *et al.* As an additional check, we measured the TO cross section at 80 K at several zone centers in the $[hhl]$ zone. Because the TO cross section at 80 K is greatly diminished by the Bose factor, we were unable to perform a quantitative comparison of the phonon intensities to the dynamic structure factors using Eq. (6). However, we find that the TO-phonon cross section at (111) is quite small. This observation agrees qualitatively with the calcula-

tions of Hirota *et al.*[11] using $S=1.5$ for which $|F_{\text{inel}}(111)|^2/|F_{\text{inel}}(200)|^2=0.14$.

V. DISCUSSION

In the previous section we presented our mode-coupling analysis and demonstrated that the characteristic features of the phonon profiles in PMN can be explained by a coupling between the TO and TA modes, without need for any additional mode. This fact implies that the TO mode we observe is the ferroelectric soft mode. However our interpretation conflicts with the model proposed by Naberezhnov *et al.*[2] and later refined by Vakhrushev and Shapiro,[17] which requires an additional soft mode. To reconcile these two models, we made a careful comparison of their data with ours. We find that, where there is overlap, the data agree quite well, and that only the interpretations are different. In this section, we attempt to explain the possible reasons for this difference.

A. Naberezhnov-Vakhrushev branch

In 1999 Naberezhnov *et al.* published an extensive study of the lattice dynamics of PMN.[2] They observed well-defined TA and low-lying TO modes in the vicinity of the (220) zone center at 800 K. Surprisingly, they found that the structure factors of the TO modes are inconsistent with those derived from the diffuse scattering intensities reported earlier by Vakhrushev *et al.*[9,10] This conclusion was based on the fact that the normalized displacements for the Pb [$\delta(\text{Pb})=1.00$], Mg or Nb [$\delta(MN)=0.18$], and oxygen atoms [$\delta(\text{O})=-0.64$], determined by Vakhrushev *et al.*[10] do not satisfy the center-of-mass condition. Naberezhnov *et al.* noted that the center of mass of the unit cell is shifted from its original position, and thus cannot correspond to optical lattice vibrations. They attributed this shift to the slow relaxation of superparaelectric clusters. They therefore concluded that the observed low-lying TO mode could not be the ferroelectric soft mode. Instead they identified it as a hard TO1 mode. A ''quasioptic'' (QO) mode was derived by fitting the TA profiles at the (200) and (110) zones to a function that couples the TA and QO modes, and this QO mode was identified as the soft mode. However, the inconsistency between the structure factors associated with the diffuse scattering and the TO mode has since been resolved by the ''phase-shifted condensed soft mode'' model proposed by Hirota *et al.*[11] Hirota *et al.* realized that the atomic displacements can be separated into two components: a uniform phase shift $\delta_{\text{shift}}=0.58$, and displacements that do satisfy the center-of-mass condition, namely $\delta_{\text{c.m.}}(\text{Pb})=0.42$, $\delta_{\text{c.m.}}(MN)=-0.40$, and $\delta_{\text{c.m.}}(\text{O})=-1.22$. Moreover, these center-of-mass displacements are consistent with the observed phonon cross section in that they correspond to a TO mode that is a mixture of Slater and Last modes in the ratio $S=1.5$. Thus, the ''phase-shifted condensed soft mode'' model is able to reconcile the intensities of the TO phonon and diffuse scattering, and demonstrates that the diffuse scattering originates from the condensation of the soft TO mode.

Vakhrushev and Shapiro have since analyzed the phonon profiles in the (300) zone where the TA-phonon cross section is expected to be extremely weak as a result of a small dynamic structure factor. Their analysis uses a function that couples the TO and QO modes and neglects the TA cross section because it was expected to be weak.[18] But as demonstrated in Fig. 3(b) and in the Appendix, the coupling between modes greatly enhances the TA-phonon cross section in spite of the small structure factor. Thus the TA mode is not negligible. The data taken by Vakhrushev and Shapiro[19] show peaks that are completely identical to the TA peaks we observe. For example, they observe a peak at ≈ 2 meV at (3,0.075,0) at 880 K (Fig. 3 in Ref. 17), which is completely consistent with the TA peak we observe in Fig. 4(b). Another data of the identical sample at $(3,-0.1,0)$ at 880 K is also published in Fig. 3 of Ref. 4. However, these peaks were treated as a ''Bragg tail''[20] in the analyses of Ref. 17. Again, the TA cross section is enhanced by the coupling and therefore one cannot neglect the TA cross section even though the structure factor for the TA mode in the (300) Brillouin zone is very small. Our model of coupling between TA and TO modes describes all of the characteristics of the phonon profiles and thus removes the need for an additional QO branch.

B. Dielectric constant

Because the QO mode is an artifact of the mode-coupling cross section, the Curie-Weiss behavior of the static dielectric constant must come from the softening of the zone-center TO mode. Therefore this TO mode is the ferroelectric soft mode. In fact, the zone-center TO mode measured at (200) exhibits a significant temperature dependence as shown in Fig. 1, and the linear temperature dependence of $(\hbar\omega_0)^2$ shown in Fig. 1(b) is qualitatively similar to that observed in conventional soft-mode ferroelectrics, such as $PbTiO_3$.[21] However, the temperature dependence of $(\hbar\omega_0)^2$ in Fig. 1(b) does not satisfy the Lyddane-Sachs-Teller (LST) relation

$$1/\epsilon \propto (\hbar\omega_0)^2, \tag{8}$$

where ϵ represents the static dielectric constant. Measurements of ϵ by Viehland *et al.*[22] for $T \geqslant 600$ K show that the static dielectric constant exhibits a Curie-Weiss behavior

$$\epsilon \propto 1/(T-T_0), \tag{9}$$

with $T_0=400$ K, which is shown by the dotted line in Fig. 1(b). On the other hand, a linear extrapolation of $(\hbar\omega_0)^2$ for $T>T_d$ gives $T_0 \approx 0$ K. This was pointed out by Vakhrushev and Shapiro in Ref. 17. We have since reanalyzed the data and confirmed that the temperature dependence of $(\hbar\omega_0)^2$ indeed follows the solid line shown in Fig. 1(b).

Vakhrushev and Shapiro found that $T/I(T)$ for $T>T_d$ varies as $T-T_0$ with $T_0=340$ K, where $I(T)$ is the integrated intensity measured at (3,0,0) over the energy range $2<\hbar\omega<12$ meV. We have performed a similar analysis on our data measured at the (200) zone center, which shows well-defined TO peaks. We fit the (200) zone center phonon profiles to a resolution-convoluted cross section composed of a Gaussian component to describe the elastic ($\hbar\omega=0$) scattering plus a damped harmonic oscillator function to describe the TO mode. The fits to the data at 1100 and 700 K are shown in the

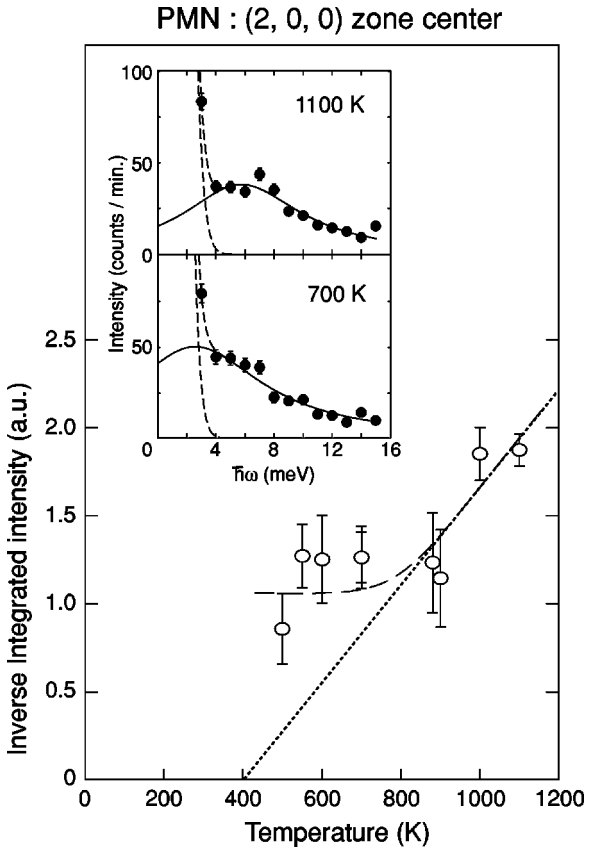

FIG. 6. Temperature dependence of the inverse integrated intensity of the zone-center TO phonon. The inset shows TO-phonon profiles measured at 1100 and 700 K. The solid and dashed lines correspond to a damped harmonic oscillator description of the TO mode and a Gaussian form centered on $\hbar\omega_0=0$, respectively (see text). The inverse integrated intensities are calculated from a numerical summation of the TO spectral weight corrected for the Bose factor. The high-temperature data ($T>800$ K) agree with the Curie-Weiss behavior measured by Viehland *et al.*, shown by the dotted line, for which $1/\epsilon \propto (T-T_0)$, where $T_0=400$ K.

insets to Fig. 6. The solid lines represent the damped harmonic oscillator component. We next evaluated the Bose-factor-corrected integrated intensity for the damped harmonic oscillator component by numerical summation. Figure 6 shows the temperature dependence of the inverse integrated intensity so obtained. The high-temperature data agree with the Curie-Weiss behavior of $1/\epsilon$ reported by Viehland *et al.* with $T_0=400$ K, which is shown as a dotted line in Fig. 6.

C. Concluding remarks

We have established the coupled nature of the TA and TO modes in PMN at 690 K, which lies above the Burns temperature T_d. This coupling, along with the soft character of the TO mode, leads naturally to the idea of a soft *coupled optic mode* that condenses at T_d, and which therefore contains a significant transverse acoustic component. This idea was originally suggested by Yamada.[23] The condensation of such a coupled optic mode would then provide an elegant explanation for the origin of the phase-shifted condensed soft mode model of the PNR proposed by Hirota *et al.*[11] If correct, this concept may be the key to understanding the fundamental mechanism underlying the unusual relaxor behavior. We have not as yet established a definite connection between such a soft coupled TO mode and the phase-shifted condensed soft mode. However, this is one of our future projects.

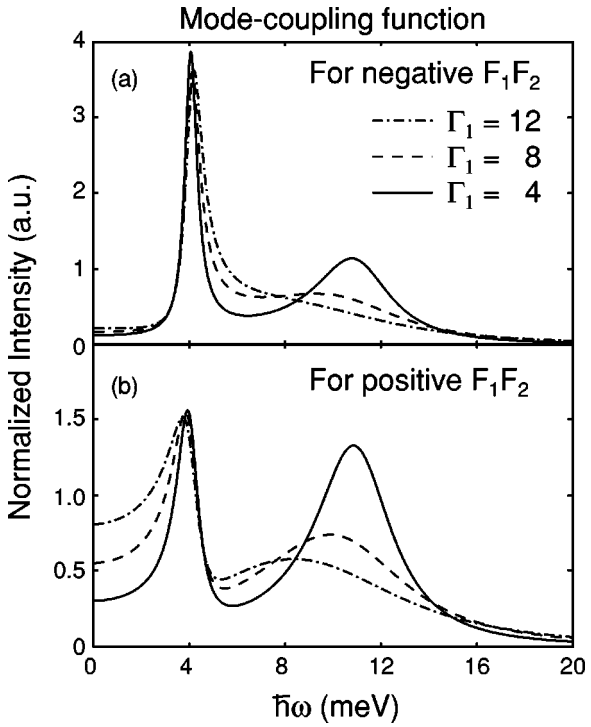

FIG. 7. Mode-coupling profiles as a function of Γ_1 with (a) $F_1F_2=-2$ (negative), and (b) $F_1F_2=85$ (positive). The other parameters were held fixed at the values $\Omega_1=11$, $\Omega_2=4$, $\Gamma_2=1$, and $\lambda=20$, which correspond to those obtained for $(2,0,-0.2)$ and $(3,0,-0.2)$. For negative F_1F_2, the spectral weight of the damped TO mode shifts toward the region between the TA and TO modes, and causes the apparent TA peak position to move to higher frequency. On the other hand, for positive F_1F_2, the spectral weight tends to shift towards the elastic ($\hbar\omega=0$) position, and this causes the apparent TA peak position to move to lower frequency.

ACKNOWLEDGMENTS

Stimulating conversations with Y. Yamada provided us with one of the key concepts presented in this paper. We also gratefully acknowledge S. B. Vakhrushev and S. M. Shapiro for sharing their data prior to publication, and we thank R. J. Birgeneau, A. A. Bokov, K. Hirota, and J. -M. Kiat for interesting discussions. Work at the University of Toronto was supported by the Natural Science and Engineering Research Council of Canada. Finally, we acknowledge financial support from the U. S. DOE under Contract No. DE-AC02-98CH10886, and the Office of Naval Research under Grant No. N00014-99-1-0738.

APPENDIX

The phonon cross sections presented here have all been fitted using the MC function [Eqs. (2), (3), and (4)] given by Harada *et al.*[12] In this appendix we present several important features of the MC function that give rise to large differences in the phonon profiles measured in different Brillouin zones.

The effects of coupling can vary substantially when the sign of F_1F_2 is changed. Figure 7 shows the cross sections calculated using the MC function. The product of the two dynamic structure factors F_1F_2 was set to be -2 (negative) for Fig. 7(a), and 85 (positive) for Fig. 7(b). In both figures three cross sections are plotted for $\Gamma_1=12$, 8, and 4, while the other parameters are fixed at $T=690$ K, $\Omega_1=11$ meV, $\Omega_2=4$ meV, $\Gamma_2=1$ meV, and $\lambda=20$. These parameters are approximately the same as those for obtained from fits to data measured for $\mathbf{Q}=(2,0,-0.2)$ and $(3,0,-0.2)$. The intensities have been normalized so that the integrated cross section is kept constant. The TO-phonon cross section for negative F_1F_2 shifts increasingly to the energy region between the TA and TO modes with increasing Γ_1. On the other hand, the TO-phonon spectral weight shifts to the energy region below the TA mode near $\hbar\omega=0$ for positive F_1F_2. Because of this, the apparent TA peak position tends to shift to higher energy for negative F_1F_2, and to lower energy for positive F_1F_2. Thus, a change in the sign of F_1F_2 causes the apparent TA peak position to shift in different directions.

Another important effect of the mode coupling is shown in Fig. 8, which displays MC cross sections for $\lambda=0$, 5, and 10. The other parameters are fixed at $T=690$ K, $\Omega_1=10$, $\Omega_2=3$, $\Gamma_1=8$, $\Gamma_2=1$, and $F_1/F_2=24$. Again the cross sections have been normalized to keep the integrated cross section constant. As a result of the coupling between modes, the TO cross section is partially transferred to the TA cross section. With sufficiently large values of λ, a remarkably large enhancement of the TA peak can occur.

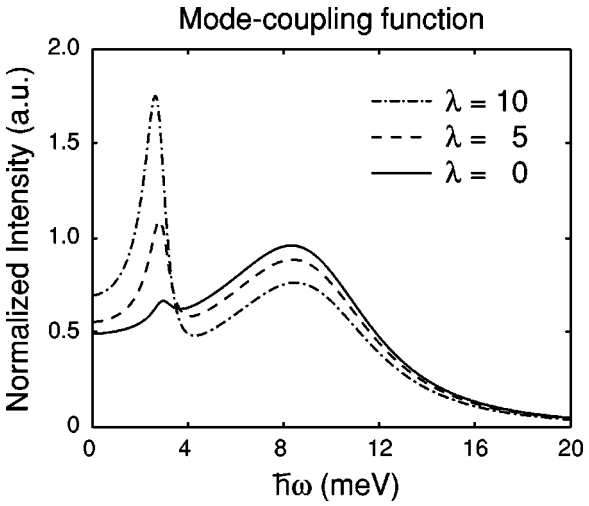

FIG. 8. Mode-coupling profiles as a function of λ. Values for the other parameters were held fixed at $\Omega_1=10$, $\Omega_2=3$, $\Gamma_1=8$, $\Gamma_2=1$, and $F_1/F_2=24$, which correspond approximately to those obtained at $\mathbf{Q}=(3,0,-0.12)$ in Fig. 4(a). Part of the TO-phonon intensity is shown to transfer to the TA mode as a result of the coupling, and results in a substantial enhancement of the TA mode intensity.

*Corresponding author.
Electronic address: waki@physics.utoronto.ca

[1] See review article, Z.-G. Ye, Key Eng. Mater. **155-156**, 81 (1998).
[2] A. Naberezhnov, S. Vakhrushev, B. Doner, D. Strauch, and H. Moudden, Eur. Phys. J. B **11**, 13 (1999).
[3] P.M. Gehring, S.-E. Park, and G. Shirane, Phys. Rev. Lett. **84**, 5216 (2000).
[4] P. M. Gehring, S. B. Vakhrushev, and G. Shirane, in Proceedings of Fundamental Physics of Ferroelectrics, Aspen, 2000 (unpublished).
[5] P.M. Gehring, S.-E. Park, and G. Shirane, Phys. Rev. B **63**, 224109 (2000).
[6] P.M. Gehring, S. Wakimoto, Z.-G. Ye, and G. Shirane, Phys. Rev. Lett. **87**, 277601 (2001).
[7] S. Wakimoto, C. Stock, R.J. Birgeneau, Z.-G. Ye, W. Chen, W.J.L. Buyers, P.M. Gehring, and G. Shirane, Phys. Rev. B **65**, 172105 (2002).
[8] G. Burns and F.H. Dacol, Solid State Commun. **48**, 853 (1983).
[9] S.B. Vakhrushev, B.E. Kvyatkovksy, A.A. Naberezhnov, N.M. Okuneva, and B. Toperverg, Ferroelectrics **90**, 173 (1989).
[10] S.B. Vakhrushev, A.A. Naberezhnov, N.M. Okuneva, and B.N. Savenko, Fiz. Tverd. Tela (St. Petersburg) **37**, 3621 (1995) [Phys. Solid State **37**, 1993 (1995)].
[11] K. Hirota, Z.-G. Ye, S. Wakimoto, P.M. Gehring, and G. Shirane, Phys. Rev. B **65**, 104105 (2002).
[12] J. Harada, J.D. Axe, and G. Shirane, Phys. Rev. B **4**, 155 (1971).
[13] N de Mathan, E. Husson, G. Calvarin, J.R. Gavarri, A.W. Huwat, and A. Morell, J. Phys.: Condens. Matter **3**, 8159 (1991).
[14] C.-S. Tu, V. Hugo Schmidt, and I.G. Siny, J. Appl. Phys. **78**, 5665 (1995).
[15] B. Dkhil, J.M. Kiat, G. Calvarin, G. Baldinozzi, S.B. Vakhrushev, and E. Suard, Phys. Rev. B **65**, 024104 (2002).
[16] J. Harada, J.D. Axe, and G. Shirane, Acta Crystallogr., Sect. A: Cryst. Phys., Diffr., Theor. Gen. Crystallogr. **26**, 608 (1970).
[17] S.B. Vakhrushev and S.M. Shapiro, cond-mat/0203103 (unpublished).
[18] This is explicitly stated in page 3 of Ref. 17.
[19] Vakhrushev and Shapiro kindly provided us with data sets taken at several different temperatures.
[20] For details about Bragg tails, see p. 114 of G. Shirane, S. M. Shapiro, and J. M. Tranquada, *Neutron Scattering with a Triple Axis Spectrometer* (Cambridge University Press, Cambridge, 2002). We confirmed that the TA mode we observed is not a Bragg tail from the fit to the MC function. The parameter F_1 is nearly q independent. If the peak were a Bragg tail, F_1 would depend strongly on q.
[21] G. Shirane, J.D. Axe, and J. Harada, Phys. Rev. B **2**, 155 (1970).
[22] D. Viehland, S.J. Jang, L.E. Cross, and M. Wuttig, Phys. Rev. B **46**, 8003 (1992).
[23] Y. Yamada (private communication).